THE JOURNAL OF BIOLOGICAL CHEMISTRY VOL. 282, NO. 40, pp. 29504–29513, October 5, 2007

A Role for Myosin 1e in Cortical Granule Exocytosis in *Xenopus* Oocytes*[S]

Received for publication, July 16, 2007, and in revised form, August 14, 2007 Published, JBC Papers in Press, August 16, 2007, DOI 10.1074/jbc.M705825200

Cataldo Schietroma[‡], Hoi-Ying Yu[§], Mark C. Wagner[¶], Joy A. Umbach[‡], William M. Bement[§], and Cameron B. Gundersen[‡1]

From the [‡]Department of Molecular and Medical Pharmacology, David Geffen UCLA School of Medicine, UCLA, Los Angeles, California 90095, the [§]Department of Zoology, University of Wisconsin, Madison, Wisconsin 53706, and the [¶]Department of Medicine, Indiana University School of Medicine, Indianapolis, Indiana 46202

***Xenopus* oocytes undergo dynamic structural changes during maturation and fertilization. Among these, cortical granule exocytosis and compensatory endocytosis provide effective models to study membrane trafficking. This study documents an important role for myosin1e in cortical granule exocytosis. Myosin1e is expressed at the earliest stage that cortical granule exocytosis can be detected in oocytes. Prior to exocytosis, myosin1e relocates to the surface of cortical granules. Overexpression of myosin1e augments the kinetics of cortical granule exocytosis, whereas tail-derived fragments of myosin1e inhibit this secretory event (but not constitutive exocytosis). Finally, intracellular injection of myosin1e antibody inhibits cortical granule exocytosis. Further experiments identified cysteine string proteins as interacting partners for myosin1e. As constituents of the membrane of cortical granules, cysteine string proteins are also essential for cortical granule exocytosis. Future investigation of the link between myosin1e and cysteine string proteins should help to clarify basic mechanisms of regulated exocytosis.**

A recent analysis concluded that the eukaryotic myosin superfamily includes 37 discrete types of myosins that are distinguished by the auxiliary domains linked to the ATP/actin-binding core of these motor proteins (1). Although the role of vertebrate, skeletal muscle myosins is well established, the specific function of the majority of the non-muscle, unconventional myosins remains unclear. To investigate the role of individual myosins in dynamic cellular events, we initiated studies using immature oocytes and eggs of *Xenopus laevis* (2, 3). These cells have several useful advantages. (i) They harbor mRNA encoding a variety of unconventional myosins (3). (ii) They undergo distinctive structural and functional changes in response to specific signaling events, including hormone-induced maturation or the induction of cortical granule exocytosis (4–9). (iii) The large size and relative ease of manipulation of these cells facilitate biochemical and ultrastructural studies, as well as dynamic imaging experiments.

In a recent study, we observed that myosin 1c (Myo1c)[2] is involved in the compression of actin coats that surround the large endosomes that are produced in the aftermath of cortical granule exocytosis in *Xenopus* eggs (3). Because a second type 1 myosin, myosin 1e (Myo1e; see ref. 10 for nomenclature), is present in *Xenopus* oocytes, we were interested whether this motor protein also has a role during cortical granule exocytosis or the ensuing process of compensatory endocytosis. Myo1e, like other myosins-1, has an NH_2-terminal actin and ATP-binding motor domain, followed by a central calmodulin-binding IQ domain and a COOH-terminal tail. The tail is composed of a basic MyTH1 (Myosin Tail Homology 1) domain that binds anionic phospholipids, and a glycine-proline-rich MyTH2 region of unknown function (11). In addition, the tails of myosins 1e and 1f include a COOH-terminal Src homology 3 (SH3) domain that presumably is involved in protein-protein interactions (12, 13).

Here we show that *Xenopus* Myo1e rapidly relocates to the surface of cortical granules in response to stimuli that trigger exocytosis. We also demonstrate that disruption of Myo1e function leads to a suppression of cortical granule exocytosis. We also show that Myo1e binds to cysteine string protein (csp), an established component of cortical granules (14) that is associated with secretory organelles in many other systems, including neurons (15, 16). These results directly link this type 1 myosin to the control of regulated exocytosis and suggest that Myo1e functions at least in part via interaction with csp.

EXPERIMENTAL PROCEDURES

Isolation and Culturing of Oocytes—Stage II–VI oocytes (17) of *X. laevis* were isolated from fragments of ovary by treatment (2–4 h at ~22 °C) in a solution containing collagenase (3–5 mg ml^{-1}) and then in a potassium phosphate solution (which facilitates the removal of the follicle cell layer) followed by culturing in Barths solution (in mM: NaCl, 88; KCl, 1; $NaHCO_3$, 2.4; Hepes, 15; $CaNO_3$, 0.3; $CaCl_2$, 0.41; $MgSO_4$, 0.82 with enrofloxacin at 10 μg/ml) as described (18). Except for Fig. 1, all experiments used stage V–VI oocytes.

Affinity Purification of Myo1e Antibody—Rabbit antisera were produced against the deduced NH_2-terminal peptide

* This work was supported by National Institutes of Health Grants GM52932 (to W. M. B.) and NS31934 (to J. A. U.). The costs of publication of this article were defrayed in part by the payment of page charges. This article must therefore be hereby marked "*advertisement*" in accordance with 18 U.S.C. Section 1734 solely to indicate this fact.

[S] The on-line version of this article (available at http://www.jbc.org) contains a supplemental movie.

[1] To whom correspondence should be addressed. Tel.: 310-825-3423; Fax: 310-206-8975; E-mail: cgundersen@mednet.ucla.edu.

[2] The abbreviations used are: Myo1c, myosin 1c; Myo1e, myosin 1e; Csp, cysteine string protein; MyTH, myosin tail homology; SH3, Src homology 3; PMA, phorbol 12-myristate 13-acetate; MBP, maltose-binding protein; eGFP, enhanced green fluorescent protein.

(MGSKERYHWQTQNVRQSGVDD**C**, where the **C** residue was for conjugation to keyhole limpet hemocyanin) or the deduced COOH-terminal peptide (**C**GWWQGRIRGREGLF-PGNYVEKI, again the **C** residue was used to conjugate the peptide to keyhole limpet hemocyanin) of *Xenopus* Myo1e. Myo1e antibody was affinity-purified by individually conjugating these peptides to Sulfolink resin (Pierce) following the manufacturer's instructions. Antiserum was adsorbed to the peptide affinity resin followed by washing with phosphate-buffered saline (PBS, in mM: NaCl, 150, KCl, 5, $NaHPO_4$, $KHPO_4$) until the A_{280} of the wash solution was <0.05. Bound antibody was eluted using 0.1 M glycine-HCl (pH 2.9), and the pH was neutralized using Tris base. Samples were concentrated to >1 mg ml^{-1} and stored in 50% glycerol at −20 °C. Identical procedures were used to obtain affinity-purified antibody targeting the COOH-terminal peptide of *Xenopus* myosin 1d (the peptide immunogen was CKINQSQPQFTKNRAGFTLSVPAN).

Subcellular Fractionation of Oocytes—Oocytes (5–10) were gently dispersed by repeated passage (6–9 times) through a yellow pipette tip using 20 μl per cell of a solution of 0.25 M sucrose, 10 mM Hepes (pH 7.4), 1 mM EGTA, and 2 mM $MgCl_2$. This homogenate was centrifuged for 3 min at ~700 × *g*, and samples of the supernatant and pellet were retained for immunoblot analysis. The supernatant was centrifuged at 100,000 × *g* for 1 h at 4 °C, and samples of the supernatant and pellet were recovered for immunoblot analysis as described below.

Generation of Myo1e Constructs for Oocyte Expression—The full-length cDNA for *Xenopus* Myo1e (GenBank™ accession number BC046842) was subcloned into the *Xenopus* transcription vector pCS2+ with or without enhanced green fluorescent protein (eGFP) upstream of the construct, as described before (19). Truncations of the full-length Myo1e included the head (residues 1–661), IQT (residues 662–1094), tail (residues 716–1094), and SH3 (residues 999–1094). Plasmid DNAs were linearized using NotI, and RNA was transcribed using the SP6 mMessage Machine (Ambion). After LiCl precipitation, the RNA was adjusted to ~1 mg ml^{-1} and oocytes were injected with 40–50 nl of the RNA solution and cultured 1–3 days prior to secretion assays or dynamic imaging.

Measurement of Cortical Granule Exocytosis—Details of this assay are in Ref. 18. Briefly, single oocytes are incubated in 10–15 μl of solution containing phorbol 12-myristate 13-acetate (PMA) at 20 or 50 nM. After 30 min (or 20 min in Fig. 7), this solution was recovered and subjected to SDS-PAGE under reducing conditions followed by Coomassie staining. The released cortical granule lectin (typically, 1–1.5 μg per oocyte; see Ref. 18) was detected principally as a broad band between 35 and 50 kDa. Where indicated, each oocyte was extracted for immunoblot analysis of Myo1e or Myo1e constructs as described for csp in Ref. 20. For Fig. 6, oocytes were injected ~4 h prior to the secretion assay with 0.5 mg of a mixture of the NH_2-terminal and COOH-terminal Myo1e antibodies or with an equivalent amount of bovine IgG (Sigma). Densitometry (three-dimensional; Eastman Kodak Co.) was used both to quantify the amount of released lectin and to compare the expression of immunoreactive Myo1e species in the oocytes. Results are given as the mean ± S.E., and statistical analyses used the Student's *t* test.

Measurement of Constitutive Exocytosis—Oocytes were injected with mRNA encoding a secreted form of alkaline phosphatase (21) with or without mRNA for Myo1e-IQT. After 2 days, individual oocytes were placed in tubes with 20–40 μl of Barths solution. After incubation for another 2–3 days, alkaline phosphatase activity was measured (as in Ref. 21) both in the medium surrounding the oocyte and in oocyte extracts. Constitutive secretion of the alkaline phosphatase was normalized to the total enzyme present (secreted enzyme plus enzyme in the cell extract) and expressed as a percentage.

Immunofluorescence Microscopy and Immunoblot Analysis of Oocytes—Oocytes were fixed (at 22 °C) in freshly prepared 3% paraformaldehyde in buffer A (0.1 M KCl, 1 mM $MgCl_2$, 1 mM EGTA, and 10 mM Hepes (pH 7.4)). After 1 h, Triton X-100 was added to 0.5%, and the cells were left in this solution for 2–3 h. Following three washes with buffer A, the oocytes were cut in half and blocked (15–30 min) using 10% goat serum in buffer A. Primary antibody was diluted in the block solution (5 μg ml^{-1} of affinity-purified Myo1e antibody targeting the COOH end or a 1:1000 dilution of Csp antiserum) along with 5 μg ml^{-1} rhodamine-conjugated *Dolichos bifluros* lectin (Vector Laboratories; this lectin binds to the cortical granule lectin of the oocyte; see Ref. 19). After 12–16 h in primary antibody (at 4 °C), the oocytes were washed with buffer A (for 2–3 h) and incubated for 2 h with Alexa-488 secondary antibody (from Molecular Probes; 2 μg ml^{-1} in block solution) followed by washing with buffer A (for 12–16 h at 4 °C). Frozen sections (10–15 μm) were cut, and epifluorescence images were obtained using an Olympus BX60 microscope with ×10 (0.40 na) or ×40 (0.85 na) objective lenses and an Olympus C-2020Z digital camera. Confocal images (1024 × 1024 pixels) were obtained using a Zeiss 510 Meta laser scanning confocal microscope equipped with a ×100, 1.3 na Pan-Neofluar objective and using 495 nm excitation (with a 505–550 bandpass filter) for the Alexa Fluor and 543 nm excitation (with a 560 nm long pass filter) for rhodamine.

Immunoblot analyses of detergent extracts of oocytes were performed as described previously (20) using either 0.2 μg ml^{-1} Myo1e antibody (described above) or Csp antibody (at 0.2–0.5 μg ml^{-1}; as described in Ref. 22) or a 1:1000 dilution of cortical granule lectin antiserum (a kind gift from Dr. J. Hedrick, University of California, Davis). The extract of *Xenopus* brain that served as a control in Fig. 1 was prepared by homogenizing whole frog brain in 0.3 M sucrose and centrifuging 10 min at 1,000 × *g*. The supernatant from this centrifugation was dispersed using concentrated electrophoresis sample buffer and used for immunoblot analysis.

Dynamic Confocal Fluorescence Microscopy and Image Analysis—Experiments were performed as described previously (3, 19). Briefly, oocytes were injected with mRNA encoding eGFP-Myo1e (~50 ng), and the next day a single oocyte was mounted on the stage of a Zeiss Axiovert 100 M microscope (with Bio-Rad 1024 × 1024 lasersharp confocal software using a numerical aperture 1.4, ×63 objective lens) in a solution containing 0.1 mg ml^{-1} wheat germ agglutinin (to suppress cortical flow), the extracellular marker, neutral, Texas Red dextran (0.1 mM; 3,000 kDa; Molecular Probes), and 50 nM PMA. The time-lapse images were collected at 2-s intervals from a single optical

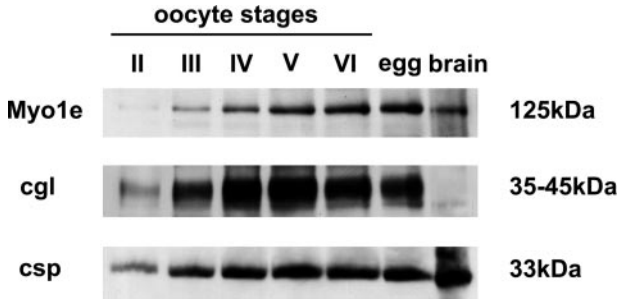

FIGURE 1. **Developmental expression of Myo1e, cortical granule lectin, and csp in frog oocytes and eggs.** Detergent extracts were prepared from oocytes (and eggs) staged according to Ref. 17. Extract from a single oocyte (or egg) was resolved electrophoretically (along with the equivalent of 50 μg of frog brain protein) for immunoblot analysis as described under "Experimental Procedures." Approximate masses of these proteins (*cgl* is cortical granule lectin) are given in kDa.

plane immediately beneath the plasma membrane. Movies were assembled and analyzed using Volocity (Improvision).

Immunoprecipitation Experiments—Extracts were prepared by homogenizing oocytes in 10 volumes of buffer A (with 190 Triton X-100) and centrifuging for 1 min at 15,000 × *g*. The lipid at the top of the extract was removed, and the centrifugation and lipid aspiration steps were repeated (2–3 times) to obtain a lipid-free solution. Extract equivalent to 20–25 oocytes was incubated at 4 °C for 12–16 h with 5–7 μg of Myo1e antibody (and either no antibody or Myo 1d antibody as a control) or 5 μl of csp antibody (prepared as in Ref. 22) followed by 1 h with 15 μl of protein A/G-agarose (Santa Cruz Biotechnology). The agarose beads were washed three times with buffer A and suspended in sample buffer for SDS-PAGE and immunoblot analysis as described in Ref. 20. Attempts to determine whether calmodulin co-immunoprecipitates with Myo1e were hampered by the lack of a suitable calmodulin antibody.

Pulldown Experiments—Full-length *Xenopus* Csp was fused to maltose-binding protein (MBP) and the recombinant fusion protein was harvested from bacterial lysates by binding to amylose resin as described in the supplier's instructions (New England Biolabs). The equivalent of ~0.1 mg of MBP-Csp or MBP alone (bound to the amylose resin) was incubated for 12–16 h at 4 °C with an oocyte extract prepared as for the immunoprecipitations (above). Alternatively, full-length Myo1e (or Myo1c) was translated in a wheat germ extract (Promega), and 20 μl of the *in vitro* translation reaction was diluted into 180 μl of buffer A (without Triton X-100) and incubated 12–16 h at 4 °C with ~0.1 mg of MBP-csp or MBP alone. The resins were washed three times with 0.5 ml of buffer A and suspended in sample buffer for immunoblot analysis. Myo1c was detected using the M2 monoclonal antibody (23).

RESULTS

Evidence that Myo1e is expressed in *Xenopus* oocytes was initially obtained by affinity-purifying antibody against the deduced NH_2- or COOH-terminal peptides of *Xenopus* Myo1e and using these antibodies for immunoblot analysis of oocyte extracts. The data reveal (Fig. 1) that Myo1e is detectable not only in fully grown stage VI oocytes (staged according to Ref. 17) but in every stage examined (stage II–VI and eggs). The increased expression of Myo1e in later stage oocytes largely parallels the expression of two other proteins: the Csp (a protein associated principally with the membrane of cortical granules in these cells; see Ref. 14), and the major cargo protein of cortical granules, cortical granule lectin (24, 25) (Fig. 1, *cgl*). Concurrently, both Myo1e and Csp are detectably expressed in *Xenopus* brain, whereas cortical granule lectin is not (Fig. 1). As a counterpoint to the Myo1e results, we observed that even though oocytes contain mRNA for myosins 1d and 1f (3), they do not detectably express either of these myosins, as judged by immunoblot analysis (data not shown).

Although type 1 myosins are predominantly globular proteins with no predicted transmembrane segments, their primary structure includes the MyTH1 domain, a region that binds to anionic phospholipids and is important for the association of these proteins with membranes (11). Thus, we were interested in determining the relative distribution of Myo1e between cytosolic and membrane compartments in the oocyte. As a first step, we used subcellular fractionation. Previous work (14) showed that when oocytes were gently disrupted in an isosmotic solution, both the plasma membrane and cortical granules (along with pigment granules and yolk platelets) sedimented during a low *g* centrifugation. By subjecting oocytes to this fractionation scheme, we found >90% of the endogenous Myo1e in the low speed supernatant (Fig. 2*A*). At the same time, all of the detectable β-tubulin was in the low speed supernatant, whereas ~90% of the csp was in the low speed pellet (Fig. 2). After ultracentrifugation of the low speed supernatant, the Myo1e remained in the high speed supernatant (as did the tubulin; Fig. 2*A*; we did not probe for csp after the ultracentrifugation). These results indicate that >90% of the Myo1e in oocytes resides in a soluble (cytosolic) compartment, whereas <10% associates with the structures that sediment at low *g* forces.

To extend the subcellular fractionation results, we used immunofluorescence microscopy to assess the distribution of Myo1e in stage VI oocytes. The image in Fig. 2*B, panel H*, reveals that at low magnification most of the immunoreactive Myo1e is detected in the cortical rim of the oocyte, where it yields a diffuse staining along with scattered brighter puncta. This cortical distribution of Myo1e immunoreactivity is similar to what is observed both for Csp (Fig. 2*B, panel D*) (14) and cortical granule lectin (which is detected using fluorescent *D. biflorus* lectin; Fig. 2*B, panel A*). At higher magnification (Fig. 2*B, panel B*), the labeling for cortical granule lectin reveals a prominent band of fluorescence that extends less than 10 μm into the interior of the oocyte and shows greatest intensity close to the plasma membrane. At the same magnification, Csp immunostaining also appears strongest in the region closest to the plasma membrane (Fig. 2*B, panel E*). However, in contrast to the lectin signal (Fig. 2*B, panel B*), the Csp immunostaining extends at least 20 μm beneath the plasma membrane (Fig. 2*B, panel E*). This trend is further accentuated for the Myo1e immunostaining, which appears as a diffuse layer extending ~50 μm into the oocyte (Fig. 2*B, panel I*). When visualized by confocal fluorescence microscopy, the staining for cortical granule lectin in an *en face* view reveals a cluster of spherical structures (~0.5–2 μm diameter) that correspond to cortical granules (Fig. 2*B, panel C*). In a similar *en face* view, Csp immunostaining is evident as a ring around many of the cortical gran-

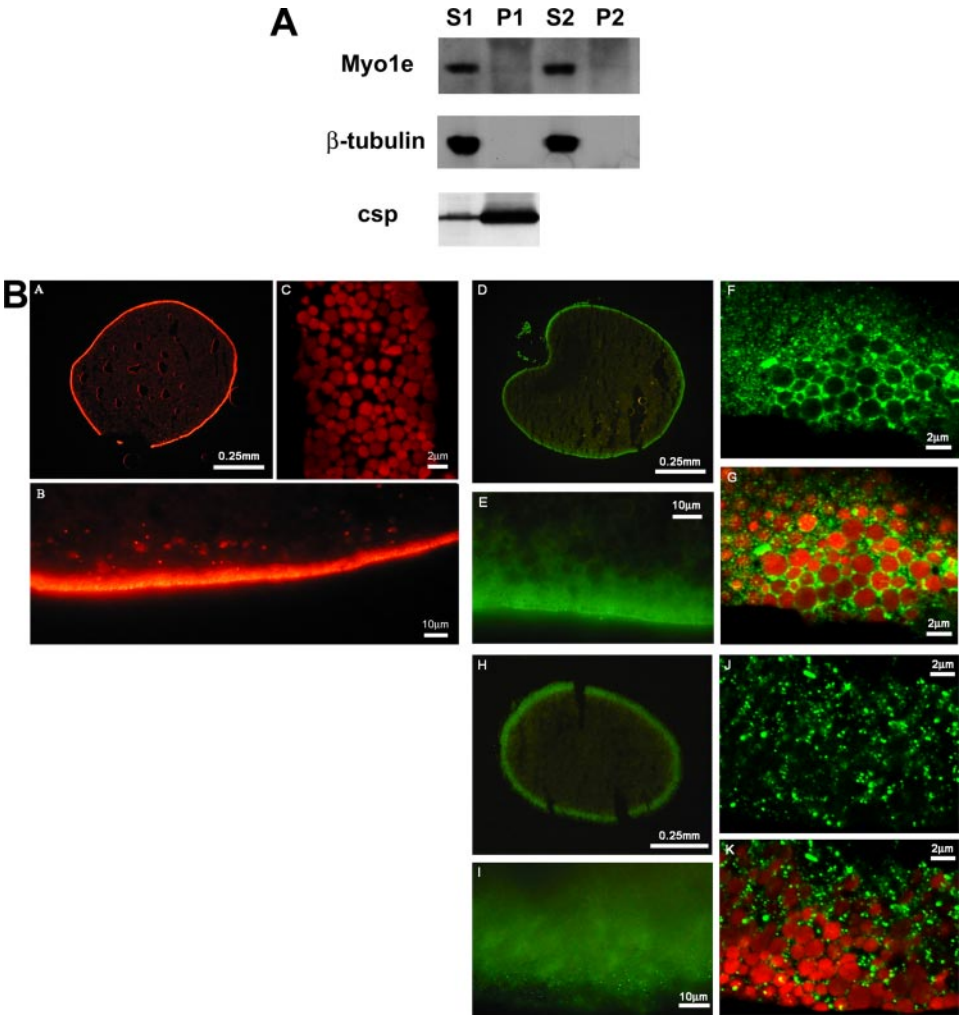

FIGURE 2. **The distribution of Myo1e in frog oocytes as revealed by subcellular fractionation and immunofluorescence microscopy.** *A,* subcellular fractionation, a homogenate of frog oocytes was subjected to low speed centrifugation (~700 × *g* for 3 min to generate supernatant 1 (*S1*) and pellet 1 (*P1*)) followed by high speed centrifugation (100,000 × *g* for 1 h to produce S2 and P2), and samples of these fractions equivalent to a single cell were subjected to immunoblot analysis for the presence of Myo1e, β-tubulin (~50 kDa), and Csp. *B,* immunofluorescence microscopy, indirect immunostaining of oocytes for Myo1e (*panels H–K*) and csp (*panels D–G*) was performed as under "Experimental Procedures," and cortical granule lectin was detected using rhodamine-conjugated *D. bifluros* lectin (*panels A–C*). By using epifluorescence microscopy at low magnification (*panels A, D,* and *H*), the signal for all three of these proteins is restricted to the cortex of the oocyte. At higher magnification, a narrow band of fluorescence is seen for cortical granule lectin (*B*). For Csp (*panel E*), the immunostaining projects deeper into the interior of the oocyte than it does for the lectin, whereas for Myo1e (*panel I*) a diffuse band of fluorescence is apparent. In *en face* views obtained using laser scanning confocal microscopy (*panels B, F, G, J,* and *K*), the *red* cortical granules are clearly identified by the binding of the *D. bifluros* lectin (*panels C, G,* and *K*). Concomitant immunostaining for Csp reveals prominent rings of labeling around granules (*panels F* and *G*). The Myo1e immunostaining (*panel J*) also is clearly apparent in the same plane as the cortical granules (*panel K*), but it is not prominently arrayed around the granules as is the Csp immunostaining.

ules (Fig. 2*B, panels F* and *G*). However, unlike Csp, Myo1e immunostaining does not encapsulate the granules (Fig. 2*B, panels J* and *K*). Instead, Myo1e immunofluorescence appears as bright puncta in the cytosolic spaces around the granules (Fig. 2*B, panels J* and *K*). Collectively, these results indicate that Myo1e is localized in the vicinity of cortical granules but that it does not significantly associate with these structures in resting oocytes.

To investigate whether Myo1e exhibits dynamic behavior during cortical granule exocytosis, we monitored the distribution of eGFP-Myo1e using time-lapse confocal microscopy. In this approach, exocytosis is triggered (by the application of PMA) in the presence of extracellular Texas Red dextran. Following exocytosis, the extracellular dextran diffuses into the lumen of the fused granules, and by focusing in a single optical plane ~1 μm beneath the plasma membrane, the entry of the dextran produces red fluorescent disks (3, 19). In the current experiments, eGFP-myo1e was detected at the plasma membrane of oocytes prior to the triggering of exocytosis (data not shown), but it was not associated with any other structures in the cortex of the cell (Fig. 3*A*, *00.00*). However, following the induction of cortical granule exocytosis, eGFP-Myo1e prominently encircled the cortical granules that had undergone exocytosis, as judged by the disc of fluorescent red dextran that was present in the same focal plane (Fig. 3*A*, *01:10*). Quantitative analysis revealed that >98% (175 of 178) of the cortical granules that underwent exocytosis had an associated ring of eGFP-Myo1e. This result strongly suggests that Myo1e participates in events that are linked to cortical granule exocytosis or the ensuing compensatory endocytosis.

Remarkably, the live imaging also revealed that in the presence of PMA, eGFP-myo1e often localized to circular compartments that lacked dextran but were of the correct dimension and in the proper location to be cortical granules (Fig. 3*A*, *01:10*). The simplest explanation of this observation is that the eGFP-myo1e relocalizes to the surface of cortical granules prior to (or during) exocytosis. Further analysis of time-lapse images confirmed this interpretation. As shown (Fig. 3*B* and supplemental movie 1), eGFP-myo1e forms annular structures well in advance of the appearance of the disks of red dextran. Quantification of the recruitment time of eGFP-myo1e relative to dextran incorporation revealed that the formation of rings of eGFP-myo1e preceded the appearance of the red dextran by 8.6 ± 0.65 s (mean ± S.E.; $n = 178$).

To ascertain whether Myo1e has a role in cortical granule exocytosis, we first evaluated the impact on this process of overexpression of the IQT region of Myo1e (see schematic in Fig. 4*C*). This approach relies on the fact that similar deletion constructs exert a dominant negative impact on events mediated by other myosins (3, 26, 27). Representative results (Fig. 4*A*) indi-

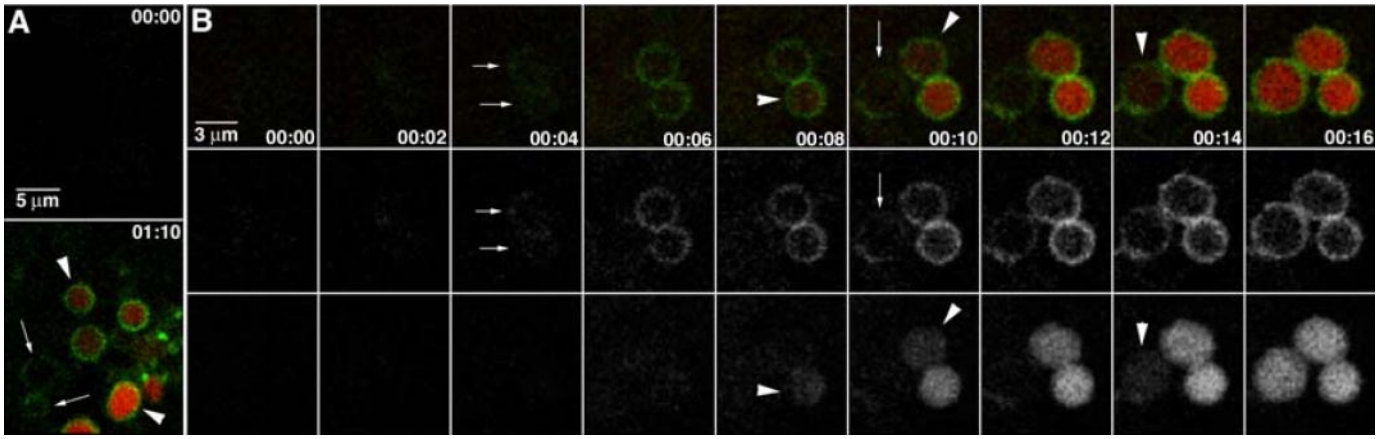

FIGURE 3. **Re-localization of eGFP-myo-1e to cortical granules.** Images are from a time-lapse, confocal movie of the sub-plasma membrane region of an oocyte induced to undergo exocytosis by PMA treatment (50 nM) in the presence of Texas Red dextran. *A,* before exocytosis (*00:00*), neither eGFP-Myo1e nor dextran is apparent. After the onset of exocytosis (*01:10*), eGFP-Myo1e (*green*) surrounds dextran (*red*), which is contained within the large endosomes generated by cortical granule-plasma membrane fusion (*arrowheads*). In addition, eGFP-Myo1e is also apparent on circular compartments of the same size but which do not contain dextran (*arrows*). *B,* eGFP-Myo1e is recruited to cortical granules prior to exocytosis. Images collected as in *A*, but at 2-s time intervals. The eGFP-Myo1e is recruited to cortical granule membranes (*arrows*) several seconds before the onset of exocytosis, as indicated by dextran filling (*arrowheads*). Time in min/s.

cate that cortical granule exocytosis is largely abolished in cells that express the IQT region of Myo1e-IQT (note that the immunoblot signal for Myo1e-IQT exceeds by >10-fold the signal for endogenous Myo1e in these cells; Fig. 4*A*). Overall, in $n = 25$ oocytes in which Myo1e-IQT expression exceeded the endogenous level of Myo1e by 12.9 ± 1.2-fold, the mean inhibition of cortical granule exocytosis was 95 ± 3% (this inhibition is significant at $p < 0.001$). This inhibitory effect of the Myo1e-IQT appears to be competitive, because as the level of overexpressed Myo1e-IQT is reduced (either by injecting less RNA for the Myo1e-IQT or by assaying cortical granule exocytosis at earlier times after RNA injection), the degree of secretory inhibition is diminished (data not shown). Thus, when Myo1e-IQT expression exceeds that of native Myo1e by >10-fold, it profoundly interferes with cortical granule exocytosis. At the same time, high level overexpression of the Myo1e-head domain has no effect on cortical granule exocytosis (Fig. 4*B*). Collectively, these data imply that one or more regions within the myo1e-IQT mediate interactions that are vital for cortical granule exocytosis.

To extend the results of Fig. 4, we evaluated whether further truncation of the Myo1e IQT yields constructs (see schematic in Fig. 4*C*) that still inhibit cortical granule exocytosis. By eliminating the calmodulin-binding IQ region, we tested the effect of the Myo1e tail. Representative results (Fig. 5*A*) indicate that high level expression of the Myo1e tail also inhibits cortical granule exocytosis. In $n = 11$ cells in which the Myo1e tail was expressed (to a mean level 9.9-fold above the immunoblot signal for endogenous Myo1e), cortical granule exocytosis was inhibited by 96 ± 2% relative to control. Next, we removed both the MyTH1 and MyTH2 domains, thereby leaving only the SH3 domain of Myo1e. This construct is highly expressed in oocytes (the signals for the SH3 domains in Fig. 5*B* exceed those of the full-length Myo1e by >27-fold), but the SH3 domain only partially inhibits (a mean reduction of 43 ± 7%) cortical granule exocytosis (Fig. 5*B*; this figure shows the greatest inhibition obtained with the SH3 domain). Thus, although the inhibitory efficacy of Myo1e-IQT is preserved in the tail construct, it is appreciably weaker in the isolated SH3 domain. Finally, note that none of the constructs of Fig. 4*C* affected the subcellular distribution of csp (judged using the fractionation procedure of Fig. 2*A*; data not shown).

As another means for perturbing cortical granule exocytosis, we investigated the effect of injecting oocytes with affinity-purified Myo1e antibody. Initially, oocytes were injected with either the affinity purified N-end or C-end antibody. Alone, these antibodies had no effect on cortical granule exocytosis, even in cells injected with 0.5 mg of purified antibody (data not shown). However, injection of oocytes with a mixture of the N-end and C-end antibody led to a nearly complete inhibition of cortical granule exocytosis (Fig. 6). These results suggest that antibodies targeting both ends of Myo1e are necessary either for the steric occlusion of Myo1e function or for the effective formation of immune complexes that prevent Myo1e from participating in exocytosis.

We also explored the possibility of inhibiting Myo1e expression in oocytes by using Myo1e-specific morpholino antisense oligonucleotides (this strategy is frequently effective for blunting protein expression in *Xenopus* embryos and other cells; see Refs. 28, 29). However, because of what appears to be a relatively slow turnover of Myo1e in oocytes (data not shown), the morpholino strategy did not result in a significant reduction of the endogenous Myo1e (data not shown). Instead, we asked whether overexpression of full-length Myo1e would enhance the kinetics of cortical granule exocytosis. For these experiments, we modified the standard cortical granule exocytosis assay (which uses 50 nM PMA and a 30-min collection period during which ~80% of the available cortical granule lectin in the cell is secreted into the medium surrounding the oocyte (14)) by using 20 nM PMA and a 20-min collection period. A representative experiment (Fig. 7) reveals that cells overexpressing full-length Myo1e exhibit a significant increase in the amount of cortical granule lectin that is discharged during this 20-min period. Overall, oocytes that overexpress Myo1e

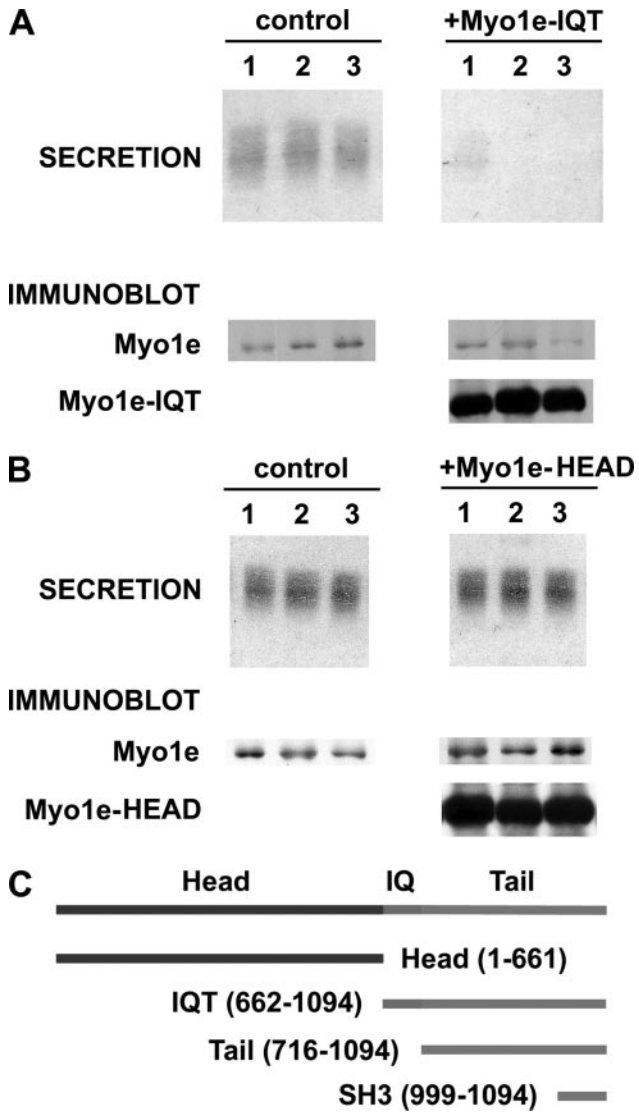

FIGURE 4. **The IQT fragment of Myo1e inhibits cortical granule exocytosis, whereas the head domain is not inhibitory.** *A,* oocytes overexpressing the Myo1e-IQT show a nearly complete inhibition of cortical granule exocytosis. The secretion data show Coomassie-stained cortical granule lectin released from three separate control oocytes (in response to PMA) along with the inhibition of this release in three cells expressing Myo1e-IQT. The immunoblot data show that Myo1e is present in control oocytes and in cells expressing Myo1e-IQT. However, only the cells injected with Myo1e-IQT mRNA express this species (~45 kDa). *B,* oocytes that overexpress Myo1e-head show no reduction of cortical granule exocytosis. The secretion data show representative results from three controls and three oocytes overexpressing Myo1e-head (as documented by the immunoblot results, which are organized as in *A*). Overall, in $n = 14$ oocytes that exhibited a 12.9 ± 1.9-fold increase in the level of Myo1e-head relative to the native Myo1e, the secretion of cortical granule lectin was 106 ± 10% of control. *C,* schematic of Myole constructs used in this paper.

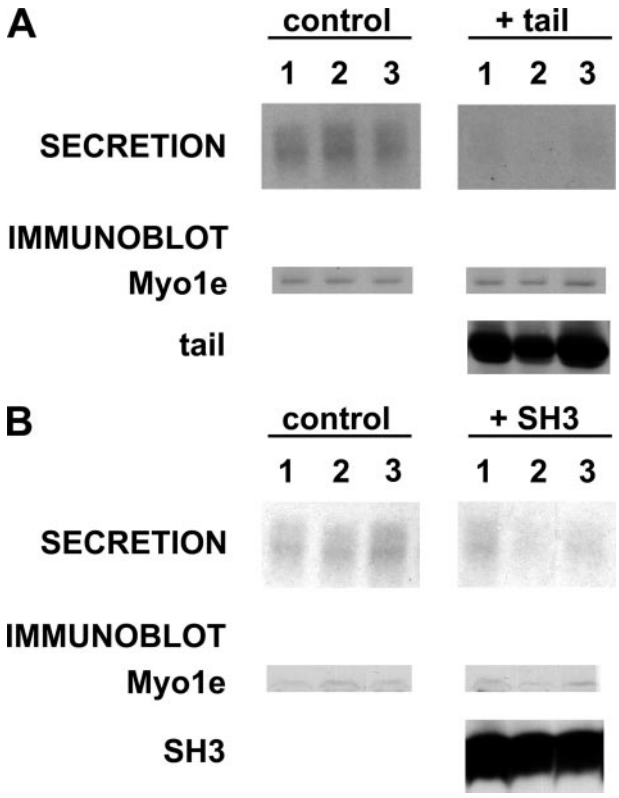

FIGURE 5. **Expression of the tail domain of Myo1e inhibits cortical granule exocytosis, whereas the isolated SH3 domain is only weakly inhibitory.** The results in *A* and *B* are organized exactly as in Fig. 4, except that they depict results from control oocytes or oocytes that overexpress either the tail region of Myo1e (~43 kDa) or the SH3 domain (12–14 kDa).

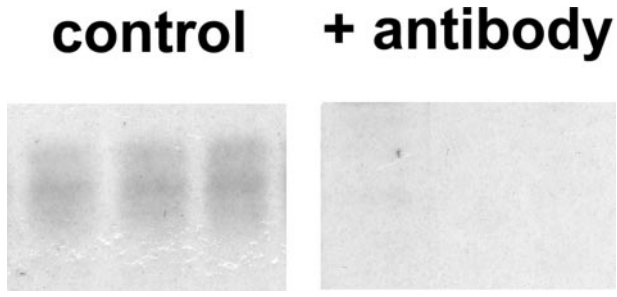

FIGURE 6. **Injection of oocytes with Myo1e antibody inhibits cortical granule exocytosis.** The results show the Coomassie-stained cortical granule lectin released from three control oocytes (injected with bovine IgG) or three oocytes injected with Myo1e antibody.

released 32 ± 6% (this difference is significant at $p < 0.01$ for $n = 15$ oocytes) more cortical granule lectin than control cells. Thus, in contrast to the significant inhibition of cortical granule exocytosis observed in oocytes expressing the tail or IQT fragments of Myo1e, overexpression of the full-length myosin enhances exocytosis.

Although the preceding data support a functional role for Myo1e in cortical granule exocytosis, we were also interested whether Myo1e participates in constitutive exocytosis. To answer this question, we overexpressed Myo1e-IQT in oocytes (under the same conditions that block cortical granule exocytosis, as shown in Fig. 4), and we monitored the constitutive secretion of alkaline phosphatase (as in Ref. 21). The results (Fig. 8) reveal that Myo1e-IQT does not inhibit the constitutive secretion of alkaline phosphatase. This finding supports the conclusion that Myo1e functions preferentially in the regulated secretory pathway.

The data of Fig. 3 indicate that PMA triggers eGFP-Myo1e to re-localize to cortical granules. Although type 1 myosins bind effectively to anionic phospholipids in bilayer membranes (11), it is assumed (30) that distinct docking/effector proteins confer specificity of type I myosins for binding to biological membranes. Thus, we sought to identify prospective binding partners for Myo1e on cortical granules. This search took into

account the following considerations. First, the evidence linking Myo1e to cortical granule exocytosis (Figs. 3–7) suggests that Myo1e might interact with one or more cortical granule proteins that participate in exocytosis. In this context, it is noteworthy that membranes of regulated secretory organelles (particularly, synaptic vesicles) include no more than ~10 distinct classes of proteins (31). Of these ~10 classes of proteins, oocytes contain no detectable synaptophysin, SV2A or -B, or synapsins (as judged by immunoblot analysis using antibodies that detect these proteins in *Xenopus* brain extracts; data not shown). Concurrently, there remains little evidence linking proteins like synaptogyrin and the SCAMPs (secretory carrier-associated membrane proteins) to steps in the exocytotic cascade (32). Although Csp and synaptotagmin I are present in *Xenopus* oocytes (14, 33), we have been unable to detect the most common vesicular-soluble, *N*-ethylmaleimide-sensitive factor attachment receptors synaptobrevins I–III in oocytes (data not shown). Thus, our search for prospective Myo1e docking proteins focused on Csp and synaptotagmin I. Using Myo1e antibody for immunoprecipitations, we tested for co-immunoprecipitation of Csp or synaptotagmin I. These experiments revealed that Csp co-immunoprecipitates with Myo1e (Fig. 9). However, there was no detectable co-immunoprecipitation of synaptotagmin I (data not shown; as additional controls, neither β-tubulin nor myristoylated, alanine-rich, protein kinase C substrate co-immunoprecipitated in these experiments). Concurrently, immunoprecipitation of Csp also culminated in co-immunoprecipitation of Myo1e (Fig. 9). These results are suggestive of a link between csp and Myo1e during cortical granule exocytosis.

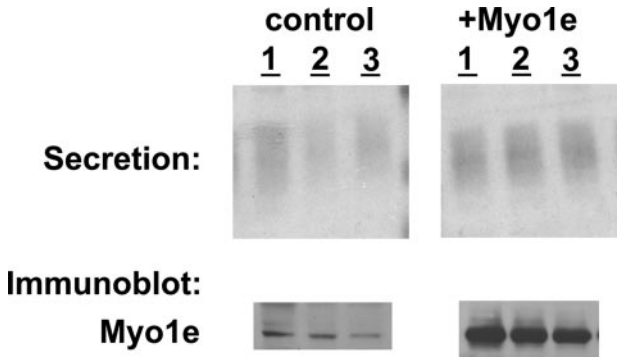

FIGURE 7. **Cortical granule exocytosis is enhanced in oocytes overexpressing Myo1e.** The secretion results show an increased release of cortical granule lectin in the three oocytes that overexpress (by >5-fold) Myo1e relative to three uninjected control cells.

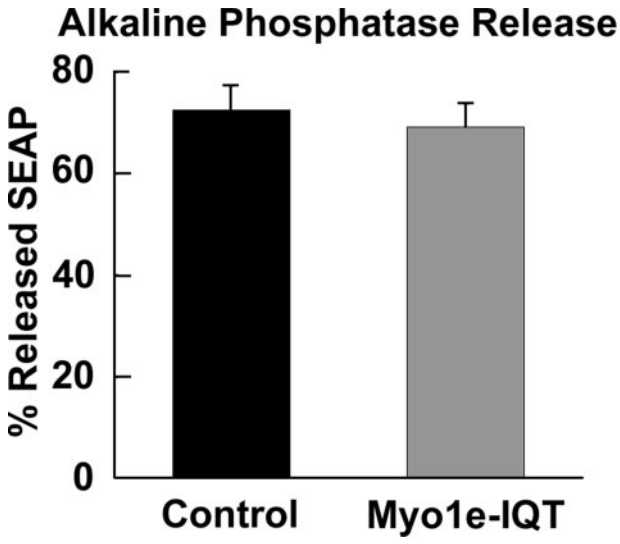

FIGURE 8. **The IQT fragment of Myo1e does not inhibit the constitutive secretion of alkaline phosphatase from oocytes.** Oocytes were injected with mRNA encoding a constitutively secreted form of alkaline phosphatase along with mRNA for Myo1e-IQT (for control cells, water replaced the Myo1e-IQT mRNA). After 2 days, the cells were arrayed individually to collect the constitutively secreted alkaline phosphatase. At the end of the collection period, the amounts of alkaline phosphatase released and retained (in the cell) were assayed. The figure presents the amount of alkaline phosphatase activity released into the medium (from control and Myo1e-IQT-expressing cells), as a percentage of the total enzyme activity (released enzyme plus the enzyme retained within the oocyte).

To extend the observations of Fig. 9, we first investigated whether the Myo1e that is present in oocyte extracts binds to immobilized, recombinant Csp. The recombinant Csp was prepared as a fusion to MBP, and the fusion construct was bound to amylose resin. Results in Fig. 10*A* indicate that Myo1e in an oocyte extract binds to recombinant MBP-Csp but not to MBP alone. Because the results in Figs. 9 and 10*A* could arise either from a direct association of Csp and Myo1e, or via an indirect interaction (mediated by some other protein in the oocyte extract), we next tested whether Myo1e binds to Csp in the absence of oocyte extract. These experiments were hampered by the poor recovery of intact Myo1e from bacterial expression systems. To circumvent this problem, we used *in vitro* translation to prepare Myo1e (as well as Myo1c and the Myo1e-head). Data in Fig. 10*B* indicate that *in vitro* translated Myo1e binds to MBP-Csp but not to MBP alone. Concomitantly, neither Myo1c nor the Myo1e-head binds to MBP-Csp (or to MBP; Fig. 10*B*). These results are consistent with a direct (and selective) interaction between Csp and Myo1e and support the conclusion from earlier experiments that determinants within the tail of Myo1e are important for exocytosis in oocytes.

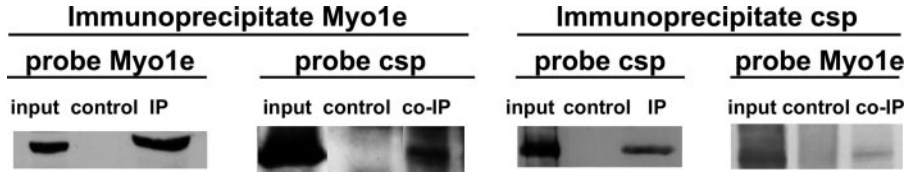

FIGURE 9. **Csp co-immunoprecipitates with Myo1e and Myo1e co-immunoprecipitates with Csp.** In each instance, the signal in the *input lane* corresponds to the immunoreactivity (for Myo1e or Csp) present in 5% of the total oocyte extract (a lipid-depleted supernatant fraction prepared from oocytes using buffer A) that was used for the immunoprecipitation (*IP*). The *control lanes* represent samples where the immunoprecipitation was done using either Myo1d antibody or no primary antibody. The *IP lanes* show the signal obtained when Csp immunoprecipitates were probed for Csp or when Myo1e immunoprecipitates were probed for Myo1e. The *co-IP lanes* show the extent of co-immunoprecipitation of either Csp (with Myo1e antibody) or Myo1e (with Csp antibody).

DISCUSSION

Several observations support the conclusion that Myo1e participates in cortical granule exocytosis in frog oocytes. First, this protein is expressed as early as stage II in these cells. By this stage, oocytes are

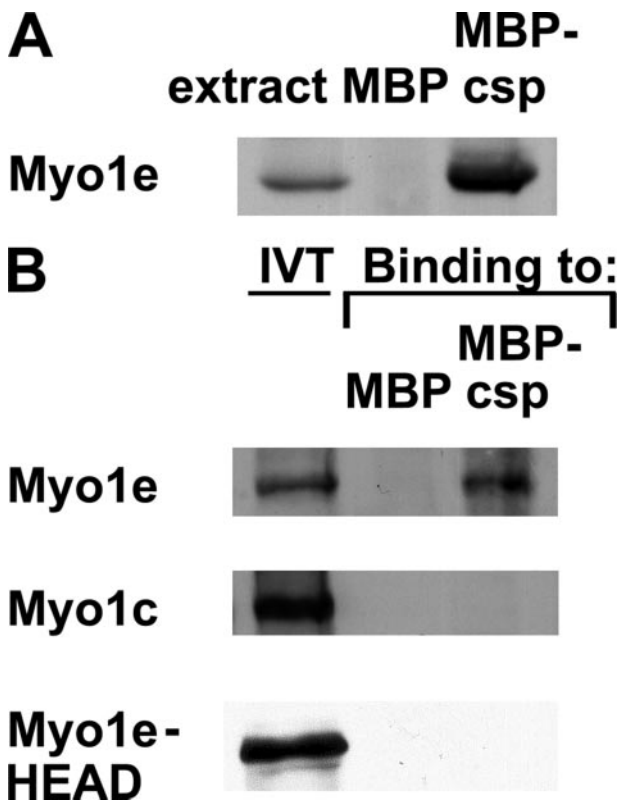

FIGURE 10. **Endogenous Myo1e from oocytes and *in vitro* translated Myo1e bind to recombinant Csp immobilized on amylose resin.** *A,* extracts from 20 oocytes were prepared as in Fig. 9 and incubated 16 h with 0.1 mg of MBP bound to amylose resin or 0.1 mg of MBP-Csp bound to amylose resin. The resins were washed with buffer A and extracted with SDS sample buffer for Myo1e immunoblot analysis. The *extract lane* reflects the Myo1e immunoreactivity in extract from a single oocyte. *B,* equivalent amounts (0.1 mg) of MBP or MBP-Csp were bound to amylose resin and incubated in a solution containing 20 μl of *in vitro* translated (*IVT*) Myo1e, Myo1e-head, or Myo1c (see "Experimental Procedures"). After washing, the resin was extracted with SDS sample buffer and subjected to immunoblot analysis. The *in vitro* translated (*IVT*) *lanes* show the immunoreactive Myo1e, Myo1e-head (~75 kDa) or Myo1c (~105 kDa), in 2.5 μl of the *in vitro* translation reaction. None of these proteins bound to amylose resin with MBP. Only Myo1e was detected bound to resin containing MBP-Csp.

already capable of secreting cortical granule lectin in response to PMA (18) indicating that they possess the molecular machinery needed for regulated exocytosis. Second, cytosolic Myo1e relocates in a stimulus-dependent fashion to the surface of cortical granules. It arrives there prior to the onset of exocytosis, implying that it may contribute to a pivotal step in the exocytotic cascade. Third, overexpression of recombinant constructs of Myo1e (which delete the motor domain or the motor domain plus the IQ region) leads to a prominent inhibition of cortical granule exocytosis (but not constitutive exocytosis). Fourth, injection of oocytes with antibody targeting the NH_2 and COOH termini of Myo1e inhibits cortical granule exocytosis. Fifth, overexpression of full-length Myo1e enhances the kinetics of cortical granule exocytosis. Collectively, these observations raise interesting questions both about the specific role of Myo1e in regulated exocytosis, as well as the mechanism of its re-localization to cortical granules.

To date, abundant evidence points to the involvement of certain unconventional myosins (particularly, type V myosins) in the transport of secretory organelles within the actin-rich cortex of cells (34–38). Thus, one possibility is that Myo1e contributes to a late stage transport step that immediately precedes (on a time scale of seconds; see Fig. 3) cortical granule exocytosis. For this hypothesis to be tenable, we need to know whether cortical granules are situated at a sufficient distance from the plasma membrane to require a pre-exocytotic transport step. In this context, it is interesting that an electron microscopic study revealed that the sub-plasmalemmal distribution of *Xenopus* cortical granules changes during the transition of an immature oocyte into a meiotically mature egg (9). Thus, during the early stages of progesterone-induced maturation, few cortical granules were within 200 nm of the plasma membrane. However, after maturation, most granules were <200 nm from the plasma membrane (9). Although these results indicate that cortical granules undergo a re-distribution during maturation, the large size of these organelles (diameters up to ~3 μm) makes it difficult to determine with accuracy the *minimum distance* between the membrane of individual cortical granules and the plasma membrane. This uncertainty derives from the fact that when oblate structures of this diameter approach a relatively planar surface (*i.e.* the plasma membrane), only a small fraction of the cortical granules will be sampled where their membrane makes its closest approach to the plasma membrane (for instance, when a 100 nm thick transverse section of the cortex of an oocyte is visualized in the electron microscope, fewer than 10% of the cortical granules will be sampled at their *closest* approach to the plasma membrane). Despite this caveat, if we assume that cortical granules are typically situated ~200 nm from the plasma membrane, then a transport step clearly becomes an essential prerequisite for exocytosis. In fact, although information is not yet available for Myo1e, the step size of Myo1c (estimated at 5–6 nm; see Ref. 39) suggests that multiple duty cycles of Myo1e would be necessary to close a 200 nm gap between a cortical granule and the plasma membrane.

Although Myo1e may be involved in a "pre-exocytotic" stage of granule transport, we cannot exclude other possible functions for this protein. For instance, Myo1e may contribute to a pre-exocytotic "bending" of the plasma membrane. Early descriptions of an inward dimpling of the plasma membrane during exocytosis included evidence for cytoskeletal elements connecting the target membranes (discussed in Ref. 40 and see recent reviews of the possible contributions of membrane bending and hemi-fusion to exocytosis; see Refs. 41, 42). However, there has been little further characterization of these cytoskeletal elements or their functional significance. It may be of interest to pursue this issue, both in the context of our results and data from several other groups that suggest that certain myosins have roles in exocytosis that are unrelated to organelle transport (43–45). However, in addition to membrane bending, other prospective functions for these "exocytotic" myosins include roles in the re-distribution of proteins on the secretory granule surface or as contributors to the dilation of the fusion pore (something that may be important in cells with secretory organelles as large as cortical granules). Clearly, additional work will be needed to clarify the role(s) of myosins in exocytosis.

The dynamic imaging data indicate that Myo1e binds to the cortical granule surface on a time scale that is consistent with

this motor protein having a role in regulated exocytosis. At the same time, the protein interaction data suggest that Csp, a protein associated with the cortical granule surface (14), may play a role as a docking or effector protein for Myo1e. In fact, the identification of docking proteins for type 1 myosins has been an elusive task (30) and has led to the possibility that the membrane association of these proteins relies principally, if not exclusively, on specific lipid targets in the membrane (46). However, it is plausible that the apparent interaction between Myo1e and Csp goes beyond a stabilization of the membrane (lipid) binding of Myo1e. Recent investigations (20) indicate that Csp, in conjunction with a 70-kDa cognate heat shock protein (Hsc70), plays an important role in cortical granule exocytosis in oocytes. Thus, although the precise contribution of Csp (and Hsc70) to the exocytotic sequence remains to be clarified, the current experiments suggest that Csp function is likely to be intertwined with that of Myo1e, and possibly serve as a model for understanding the role of myosins in exocytosis.

Prior studies of vertebrate Myo1e revealed that this myosin isoform was concentrated in the cytoplasm and in elongated structures at sites of intercellular contact that contained actin and α-actinin but not vinculin (47). In addition, Myo1e was found at intercellular adherens-type junctions that were induced by constitutively active Cdc42 (48). This targeting did not rely on the SH3 domain, but it was disrupted upon deletion of the COOH-terminal ~180 residues of Myo1e implying that this portion of the Myo1e tail was essential for its subcellular distribution (48). These latter observations offer certain parallels to the current work in that overexpression of the SH3 domain of Myo1e only weakly interferes with cortical granule exocytosis, whereas the complete tail region is an effective inhibitor of exocytosis. The most likely explanation for these results is that the MyTH1 or MyTH2 regions in the tail of Myo1e include determinants that stabilize its interaction with specific targets in the oocyte that are important not only for exocytosis but also for the subcellular localization of Myo1e. In a separate study, Myo1e was found preferentially in the cuticular plate, an actin meshwork that anchors the stereocilia in auditory and vestibular epithelia (49), and a very recent investigation implicated Myo1e in constitutive endocytosis (50). Although our data argue for an exocytotic function of Myo1e in oocytes, we cannot exclude a role in endocytosis. Regardless, in view of the diverse cell types in which Myo1e is expressed, it will be important to determine whether common mechanisms underlie the subcellular distribution and function of this motor protein.

We recently reported that Myo1c participates in the compensatory endocytosis that follows cortical granule exocytosis (3). Specifically, Myo1c is required for tight coupling of dynamic actin to the membranes of exocytosing cortical granules. Together with the current results, these findings indicate that different myosins 1 can play distinctly different roles on the same membrane compartment within a very short time span. Presumably, at least some of the variation in the roles played by these two myosins reflects differences in the structure of their tail region and associated light chains; Myo1c has three IQ motifs and three associated calmodulin light chains, in contrast to Myo1e, which has a single IQ motif and associated calmodulin. In addition, Myo1c lacks the MyTH2 and SH3 domains found in the tail of Myo1e (11).

In summary, this study indicates that Myo1e plays a vital role during regulated exocytosis (but not constitutive exocytosis) in frog oocytes. It will be interesting to determine whether Myo1e contributes to regulated secretion in other cell types and to learn more about the molecular role of Myo1e in this process.

Acknowledgments—We thank Drs. C. Sternini, N. Brecha, and H. Kornblum (UCLA) for access to the microscopes used for immunofluorescence microscopy. The acquisition of the confocal microscope used for the dynamic imaging was supported by National Science Foundation Grant NSF9724515 (to J. Pawley).

REFERENCES

1. Richards, T. A., and Cavalier-Smith, T. (2005) *Nature* **436,** 1113–1118
2. Weber, K. L., Sokac, A. M., Berg, J. S., Cheney, R. E., and Bement, W. M. (2005) *Nature* **431,** 325–329
3. Sokac, A. M., Schietroma, C., Gundersen, C. B., and Bement, W. M. (2006) *Dev. Cell* **11,** 629–640
4. Campanella, C., Andreucetti, P., Taddei, C., and Talevi, R. (1984) *J. Exp. Zool.* **229,** 283–293
5. Charbonneau, M., and Grey, R. D. (1984) *Dev. Biol.* **102,** 90–97
6. Colman, A., Jones, E. A., and Heasman, J. (1985) *J. Cell Biol.* **101,** 313–318
7. Larabell, C. A., and Chandler, D. E. (1988) *Cell Tissue Res.* **251,** 129–136
8. Bement, W. M., and Capco, D. G. (1989) *J. Cell Biol.* **108,** 885–892
9. Bement, W. M., and Capco, D. G. (1989) *Cell Tissue Res.* **255,** 183–191
10. Gillespie, P. G., Albanesi, J. P., Bahler, M., Bement, W. M., Berg, J. S., Burgess, D. R., Brurnside, B., Cheney, R. E., Corey, D. P., Coudrier, E., de Lanerolle, P., Hammer, J. A., Hasson, T., Holt, J. R., Hudspeth, A. J., Lkebe, M., Kendrick-Jones, E. D., Korn, E. D., Li, R., Mercer, J. A., Milligan, R. A., Mooseker, M. S., Ostap, E. M., Petit, C., Pollard, T. D., Sellers, J. R., Soldati, T., and Titus, M. A. (2001) *J. Cell Biol.* **155,** 703–704
11. Sokac, A. M., and Bement, W. M. (2000) *Int. Rev. Cytol.* **200,** 197–304
12. Pawson, T. (1995) *Nature* **373,** 573–580
13. Cesarini, G., Panni, S., Nardelli, G., and Castagnoli, L. (2002) *FEBS Lett.* **513,** 38–44
14. Gundersen, C. B., Aguado, F., Sou, S., Mastrogiacomo, A., Coppola, T., Kornblum, H. I., and Umbach, J. A. (2001) *Cell Tissue Res.* **303,** 211–219
15. Buchner, E., and Gundersen, C. B. (1997) *Trends Neurosci.* **20,** 223–227
16. Chamberlain, L. H., and Burgoyne, R. D. (2000) *J. Neurochem.* **74,** 1781–1789
17. Dumont, J. N. (1972) *J. Morphol.* **136,** 153–179
18. Gundersen, C. B., Kohan, S. A., Chen, Q., Iagnemma, J., and Umbach, J. A. (2002) *J. Cell Sci.* **115,** 1313–1320
19. Sokac, A. M., Co, C., Taunton, J., and Bement, W. M. (2003) *Nat. Cell Biol.* **5,** 727–732
20. Smith, G. B., Hirano, A., Umbach, J. A., and Gundersen, C. B. (2005) *J. Biol. Chem.* **280,** 32669–32675
21. Tate, S. S., Urade, R., Micanovic, R., Gerber, J., and Udenfriend, S. (1990) *FASEB J.* **4,** 227–231
22. Poage, R. E., Meriney, S. L., Gundersen, C. B., and Umbach, J. A. (1999) *J. Neurophysiol.* **82,** 50–59
23. Wagner, M. C., Barylko, B., and Albanesi, J. P. (1992) *J. Cell Biol.* **119,** 163–170
24. Nishihara, T., Wyrick, R. E., Working, P. K., Chen, Y. H., and Hedrick, J. L. (1986) *Biochemistry* **25,** 6013–6020
25. Chang, B. Y., Peavy, T. R., Wardip, N. J., and Hedrick, J. L. (2004) *Comp. Biochem. Physiol. A.* **137,** 115–129
26. Raposo, G., Cordonnier, M. N., Tenza, D., Menichi, B., Durrbach, A., Louvard, D., and Coudrier, E. (1999) *Mol. Biol. Cell* **10,** 1477–1494
27. Bose, A., Guilherme, A., Robida, S. I., Nicoloro, S. M., Zhou, Q. L., Jiang, Z. Y., Pomerleau, D. P., and Czech, M. P. (2002) *Nature* **420,** 821–824
28. Heasman, J., Kofron, M., and Wylie, C. (2000) *Dev. Biol.* **222,** 124–134
29. Heasman, J. (2002) *Dev. Biol.* **243,** 209–214

30. Barylko, B., Jung, G., and Albanesi, J. P. (2005) *Acta Biochim. Pol.* **52,** 373–380
31. Sudhof, T. C., and Scheller, R. H. (2001) *Synapses* (Cowan, W. M., Sudhof, T. C., and Stevens, C. F., eds) pp. 177–215, The Johns Hopkins University Press, Baltimore
32. Hubner, K., Windoffer, R., Hutter, H., and Leube, R. E. (2002) *Int. Rev. Cytol.* **214,** 103–159
33. Kohan, S. A., and Gundersen, C. B. (2003) *J. Exp. Zool.* **300,** 113–125
34. Provance, D. W., and Mercer, J. A. (1999) *Cell. Mol. Life Sci.* **56,** 233–242
35. Oliver, T. N., Berg, J. S., and Cheney, R. E. (1999) *Cell. Mol. Life Sci.* **56,** 243–257
36. Doussau, F., and Augustine, G. J. (2000) *Biochemie* (*Paris*) **82,** 353–363
37. Wu, X., Jung, G., and Hammer, J. A., III (2000) *Curr. Opin. Cell Biol.* **12,** 42–51
38. Langford, G. M. (2002) *Traffic* **3,** 859–865
39. Veigel, C., Coluccio, L. M., Jontes, J. D., Sparrow, J. C., Milligan, R. A., and Molloy, J. E. (1999) *Nature* **398,** 530–533
40. Mozingo, N. M., and Chandler, D. E. (1995) *Rapid Freezing, Freeze Fracture, and Deep Etching* (Severs, N. J., and Shotton, D. M., eds) pp. 285–310, Wiley-Liss, Inc., New York
41. Chernomordik, L. V., and Kozlov, M. M. (2005) *Cell* **123,** 375–382
42. Zimmerberg, J., and Kozlov, M. M. (2006) *Nat. Rev. Mol. Cell Biol.* **7,** 9–19
43. Bose, A., Robida, S., Furcinitti, P. S., Chawla, A., Fogerty, K., Corvera, S., and Czech, M. P. (2004) *Mol. Cell. Biol.* **24,** 5447–5458
44. Neco, P., Giner, D., Viniegra, S., Borges, R., Villarroel, A., and Gutierrez, L. M. (2004) *J. Biol. Chem.* **279,** 27450–27457
45. Togo, T., and Steinhardt, R. A. (2004) *Mol. Biol. Cell* **15,** 688–695
46. Hokanson, D. E., and Ostap, E. M. (2006) *Proc. Natl. Acad. Sci. U. S. A.* **103,** 3118–3123
47. Stoffler, H. E., Ruppert, C., Reinhard, J., and Bahler, M. (1995) *J. Cell Biol.* **129,** 819–830
48. Stoffler, H. E., Honnert, U., Bauer, C. A., Hofer, D., Schwarz, H., Muller, R. T., Drenckhahn, D., and Bahler, M. (1998) *J. Cell Sci.* **111,** 2779–2788
49. Dumont, R. A., Zhao, Y. D., Holt, J. R., Bahler, M., and Gillespie, P. G. (2002) *J. Assoc. Res. Otolaryngol.* **3,** 375–389
50. Krendel, M., Osterweil, E. K., and Mooseker, M. S. (2007) *FEBS Lett.* **581,** 644–650